CellPress

Developmental Cell
Article

Membrane-Bound Methyltransferase Complex VapA-VipC-VapB Guides Epigenetic Control of Fungal Development

Özlem Sarikaya-Bayram,[1] Özgür Bayram,[1,7] Kirstin Feussner,[2] Jong-Hwa Kim,[3] Hee-Seo Kim,[3,4] Alexander Kaever,[5] Ivo Feussner,[2] Keon-Sang Chae,[4] Dong-Min Han,[6] Kap-Hoon Han,[3] and Gerhard H. Braus[1,*]
[1]Department of Molecular Microbiology and Genetics, Georg August University, Grisebachstrasse 8, Göttingen 37077, Germany
[2]Department of Plant Biochemistry, Georg August University, Justus-von-Liebig-Weg 11, Göttingen 37077, Germany
[3]Department of Pharmaceutical Engineering, Woosuk University, Wanju 565-701, Korea
[4]Department of Molecular Biology, Chonbuk National University, Jeonju 561-756, Korea
[5]Department of Bioinformatics, Georg August University, Goldschmidtstrasse 1, Göttingen 37077, Germany
[6]Division of Life Sciences, Wonkwang University, Iksan 570-749, Korea
[7]Present address: Department of Biology, National University of Ireland, Maynooth, Co. Kildare, Ireland
*Correspondence: gbraus@gwdg.de
http://dx.doi.org/10.1016/j.devcel.2014.03.020

SUMMARY

Epigenetic and transcriptional control of gene expression must be coordinated in response to external signals to promote alternative multicellular developmental programs. The membrane-associated trimeric complex VapA-VipC-VapB controls a signal transduction pathway for fungal differentiation. The VipC-VapB methyltransferases are tethered to the membrane by the FYVE-like zinc finger protein VapA, allowing the nuclear VelB-VeA-LaeA complex to activate transcription for sexual development. Once the release from VapA is triggered, VipC-VapB is transported into the nucleus. VipC-VapB physically interacts with VeA and reduces its nuclear import and protein stability, thereby reducing the nuclear VelB-VeA-LaeA complex. Nuclear VapB methyltransferase diminishes the establishment of facultative heterochromatin by decreasing histone 3 lysine 9 trimethylation (H3K9me3). This favors activation of the regulatory genes *brlA* and *abaA*, which promote the asexual program. The VapA-VipC-VapB methyltransferase pathway combines control of nuclear import and stability of transcription factors with histone modification to foster appropriate differentiation responses.

INTRODUCTION

Methylation represents an important cellular posttranslational modification (PTM). Nuclear methyltransferases (MTs) target DNA or modify basic residues of histones to control gene expression, which is essential for development, various diseases, and aging (Hong et al., 2012; Yang and Bedford, 2013). Nuclear methyltransferase activity is adjusted through transduction pathways that receive external signals mostly at the plasma membrane (Good et al., 2011). Phosphorylation is the most common PTM in signal transduction, whereas there are hardly any examples of methyltransferases that directly participate in a signal transduction pathway. The mitogen-activated protein kinase (MAPK) pathways represent paradigms of signal transduction in which kinase modules are tethered to the plasma membrane and can be released to the nucleus. These phosphorelay pathways are conserved from the sexual pheromone module of the budding yeast *Saccharomyces cerevisiae* to mammalian extracellular signal-regulated kinase (ERK) pathways (Saito, 2010; Zheng and Guan, 1993).

Multicellular fungi represent amenable models in which to study differentiation with established genetic and cell biological tools. Fungal development is linked to the production of secondary metabolites (Bayram and Braus, 2012; Bayram et al., 2010). These potent, bioactive small molecules influence various physiological cellular processes and are important for human health and nutrition (Brakhage, 2013; Keller et al., 2005). Fungal development and secondary metabolism depend on environmental signals such as light, nutrition, and oxygen supply. The ascomycete *Aspergillus nidulans* initiates an asexual program that results in the release of airborne spores during illumination and simultaneously reduces the formation of sexual fruiting bodies, which represent the most complicated multicellular structures of this fungus (Rodriguez-Romero et al., 2010). Fruiting-body formation is stimulated in darkness. Reduced sexual development in light correlates with decreased levels of the nuclear *velvet* complex VelB-VeA-LaeA, which is required to activate sexual development and coordinate secondary metabolism (Bayram et al., 2008). VelB-VeA forms a heterodimer of *velvet* DNA-binding domains (Ahmed et al., 2013). VeA functions as a bridge between VelB and LaeA. LaeA methyltransferase controls the secondary metabolism and formation of Hülle cells that form a tissue to nurse growing fruiting bodies (Bok and Keller, 2004; Patananan et al., 2013; Sarikaya Bayram et al., 2010).

The *velvet* complex synchronizes sexual development and secondary metabolism by interpreting light signals transmitted through receptors. The level of the nuclear *velvet* complex depends on VeA, which binds to the light receptor phytochrome (Purschwitz et al., 2009). VeA nuclear import occurs in darkness

and is impeded by light (Stinnett et al., 2007). VeA-VelB heterodimer formation is promoted by phosphorylation of the MAPK AnFus3. Upon receiving environmental signals, the *A. nidulans* MAPK module leaves the plasma membrane, travels to the nuclear envelope, and releases AnFus3 into the nucleus. Phosphorylation of VeA is vital for fungal development and secondary metabolism (Bayram et al., 2012a).

Here, we report a signal transduction pathway that is controlled by the nuclear heterodimeric methyltransferases VipC and VapB. The VapA protein contains the membrane-tethering FYVE-like (Fab1, YTOB, Vac1, EEA) zinc finger (ZF) domain. VapA can form the membrane-bound VapA-VipC-VapB complex, which excludes the methyltransferases from the nucleus. The release of the methyltransferase heterodimer from VapA leads to their nuclear import. VipC-VapB interacts with VeA and inhibits its nuclear accumulation, which results in decreased sexual development and secondary metabolism. Nuclear VapB methyltransferase activity reduces the repressive histone 3 lysine 9 trimethylation (H3K9me3), which in turn leads to a decrease in heterochromatin foci within the nucleus. Released VipC-VapB activates the asexual differentiation program as part of a methyltransferase signal transduction pathway.

RESULTS

The *velvet* Domain Protein VeA Interacts in the Nucleus with the Methyltransferase VipC to Balance Different Developmental Programs

The fungal-specific *velvet* domain is one of the interfaces of VeA for multiple protein interactions (Bayram et al., 2012a; Bi et al., 2013; Palmer et al., 2013). This includes the VeA bridging function between VelB and the methyltransferase LaeA to form the *velvet* complex for coordination of sexual development and secondary metabolism (Bayram et al., 2008). A yeast two-hybrid (YTH) screen using VeA as a bait identified several *velvet* interacting proteins (Vips), including VipC (Figure 1A). VeA-VipC represents a second cellular interaction of VeA with a putative methyltransferase. The VipC methyltransferase shows 52% similarity to LaeA. The VeA-VipC YTH interaction was verified by coimmunoprecipitation (coIP) and bimolecular fluorescence complementation (BIFC) (Figures 1B and 1C), and was more pronounced in light than in dark (Figure S1A available online). BIFC revealed that VipC interacts with VeA in the nucleus as visualized by a monomeric red fluorescent protein fused to histone 2A (mRFP-H2A). The nuclear VeA-VipC interaction indicates a second nuclear role of VeA in addition to the trimeric VelB-VeA-LaeA complex.

VipC function was addressed by generating a *vipC* deletion. A wild-type (WT) fungus forms more sexual fruiting bodies in darkness than in light. The *vipC* mutant produced elevated numbers of sexual fruiting bodies in light, whereas no change was observed in darkness, suggesting a function in light control. However, asexual development decreased in light by 70%–75% when compared with the WT (Figures 1D and 1E). A *veA*/*vipC* double mutant exhibited a predominantly *veA*Δ phenotype, supporting the notion that *veA* is epistatic to *vipC*. This included a secondary metabolism control whereby the *veA* or *veA*/*vipC* mutant lost the potential to synthesize the mycotoxin sterigmatocystin (ST), whereas the *vipC* mutant produced the toxin as the WT (Figure 1F).

These results show that VeA might be either part of two nuclear complexes or part of a supercomplex with potential methyltransferases. Besides VelB-VeA-LaeA, VeA physically interacts with VipC. The trimeric *velvet* complex is an activator of the sexual pathway, and the putative methyltransferase VipC is required for light-dependent repression of sexual fruiting body formation, but not for secondary metabolism control.

VipC Is Part of the Plasma Membrane-Associated VapA-VipC-VapB Complex, which Releases the VipC-VapB Methyltransferase Heterodimer to the Nucleus

The VipC methyltransferase was analyzed for additional interaction partners. A functional VipC-tandem affinity purification (TAP) fusion repeatedly copurified two VipC-associated proteins, VapA and VapB (Figures 2A and 2B; Table S1). Subunits of the trimeric *velvet* complex were not recruited, suggesting that the VeA-VipC interaction is rather transient. VipC, VapA, and VapB protein sizes were similar (330–350 amino acids), and interactions were verified by tagging VapA and VapB. Both tagged proteins were able to recruit the other two subunits, supporting the presence of VapA-VipC-VapB (Figures 2C and 2D; Tables S2 and S3) in light and darkness (Figure S2).

The VapA protein contains three FYVE (Fab1, YOTB, Vac1, EEA1)-like ZF domains named after the four cysteine-rich proteins in which they were originally found (Gaullier et al., 1998). The first two ZF motifs of VapA homologs are highly conserved, whereas the third motif carries alterations in the last cysteine residue in some fungi (Figure S1B). FYVE domains are characterized by six to eight cysteine pairs. FYVE-type proteins differ from ZF domain transcription factors in that they bind to membrane lipids to function in membrane trafficking or cell signaling (Gillooly et al., 2001; Hayakawa et al., 2007). BIFC verified the cellular localization of the VapA-VipC interaction. Yellow fluorescent protein N-terminally fused to VipC (N-EYFP-VipC) MT interacted with C-EYFP-VapA ZF along the plasma membrane, which is consistent with the typical FYVE ZF feature of attaching to membranes (Figure 2E).

The domain structure of VapB differs from that of VapA. VapB shares with VipC an S-adenosyl-L-methionine (SAM)-dependent putative methyltransferase domain (Figure 2B) that includes three characteristic consecutive glycine (G) residues that are conserved in fungi (Figure S1B), plants, and humans (Kozbial and Mushegian, 2005). BIFC showed a similar decoration of the plasma membrane for VapA-VapB and VapA-VipC, supporting the notion that the VapA-VipC-VapB complex is localized at the plasma membrane. BIFC of the putative methyltransferases VipC and VapB revealed two interacting subpopulations. In addition to membrane-associated VipC-VapB, a substantial number of the cellular heteromers were localized in the nucleus (Figure 2E). This indicates that VipC-VapB, which is tethered by the FYVE ZF VapA to the fungal cellular membrane, can be released from the membrane and migrate into the nucleus. Conservation of the heterotrimeric VapA-VipC-VapB complex among fungi hints to a general methyltransferase transduction pathway between the membrane and nucleus across the fungal kingdom.

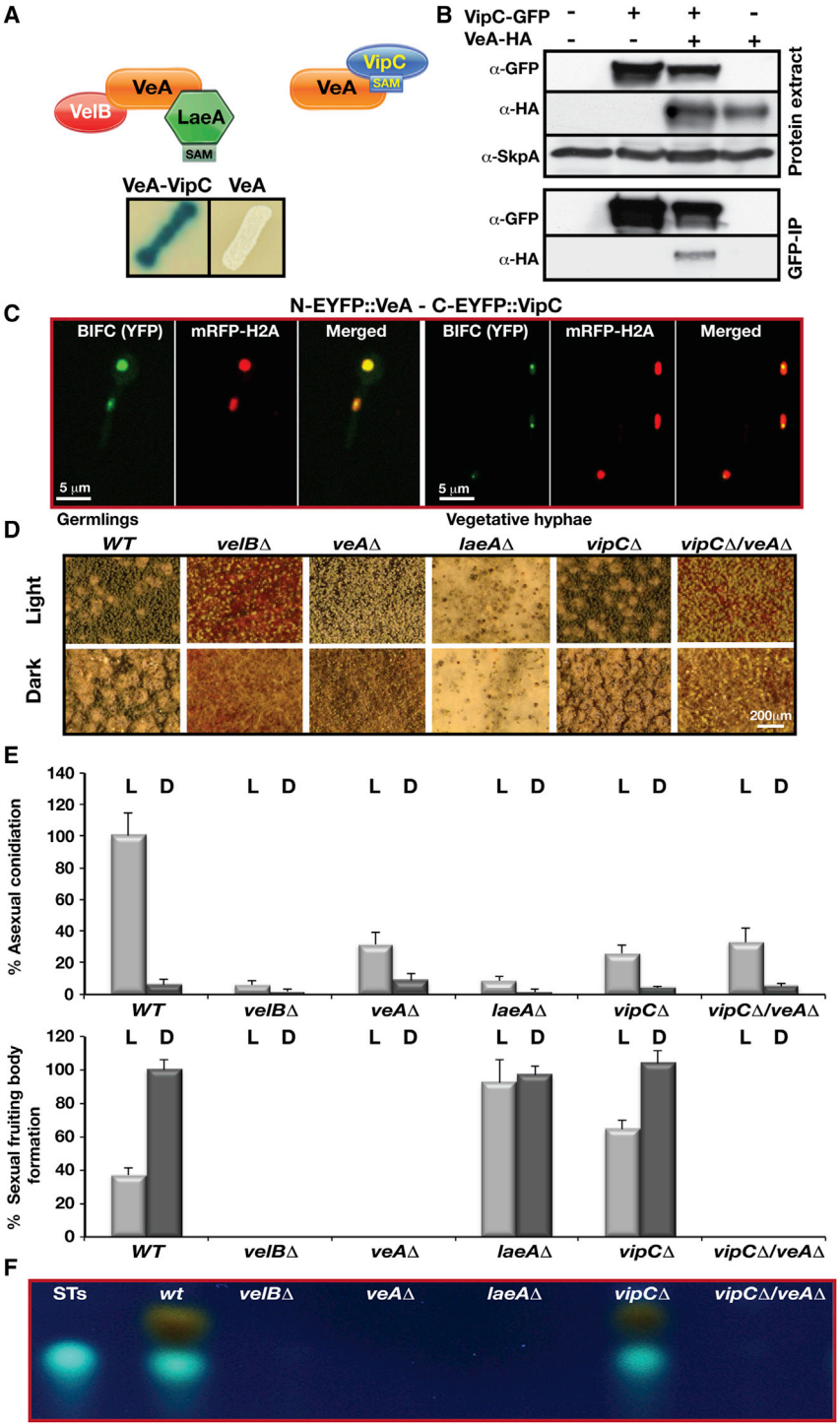

Figure 1. The Putative Methyltransferase VipC Represents a Velvet Interacting Protein

(A) Y2H screen of the VeA-interacting protein VipC, representing a putative SAM-dependent methyltransferase.

(B) CoIP of VipC-VeA interaction. VipC-GFP copurifies VeA-HA from vegetative cells grown for 24 hr at 37°C in light. α-GFP and α-HA detect tagged proteins, and α-SkpA shows equal loading.

(C) Subcellular interactions of VeA-VipC in BIFC. N-EYFP-VeA interacts with C-EYFP-VipC in the nucleus of cells grown for 16 hr at 37°C in light. Nuclei are visualized by mRFP fused to histone 2A (red).

(D and E) Comparison of *vipC*Δ and WT development. Stereomicroscopic images of the WT and *velB*Δ, *veA*Δ, and *laeA*Δ mutants together with *vipC*Δ and *vipC*Δ/*veA*Δ grown on GMM for 5 days at 37°C in light or darkness. Three sectors from independent plates were used for quantification. Conidia and fruiting bodies of WT in light or darkness represent 100%. Vertical lines represent the error bars from three different plates. *vipC*Δ showed derepressed sexual development and reduced asexual sporulation in comparison with WT.

(F) Thin-layer chromatography (TLC) of mycotoxin ST produced by WT or mutants. Only WT and *vipC*Δ produce ST. STs, ST standard.

See also Figure S1.

tive *gpdA* promoter due to the weak fluorescence signals. VipC protein did not decorate the entire membrane, but was visible as small membrane-associated dots. VipC was also present in the nucleus, where it colocalized with the mRFP-H2A. The pattern of the second methyltransferase VapB was similar to that of VipC, and both were found at the plasma membrane and in the nuclei. The ZF VapA-GFP fusion labeled the entire plasma membrane along the fungal cell, but was hardly found in the nucleus (Figure 3A). Membrane-associated VapA-GFP was in permanent motion and moved along the plasma membrane dynamically (Movie S1). The localization patterns of the complex components were independent of illumination (Figure S3). Nuclear enrichment resulted in high amounts of VipC-VapB, but only trace levels of VapA within the nucleus (Figure 3B). This supports the notion that VapA tethers the trimeric complex at the membrane and can release VipC-VapB to cross the cytoplasm and enter the nucleus.

VapA Is Predominantly a Membrane Protein, whereas the VipC and VapB Methyltransferases Are Enriched in the Nucleus

The interaction studies revealed membrane associations for VapA-VipC-VapB and nuclear interaction for the heteromeric VipC-VapB. Cellular localization of the subunits was monitored by functional GFP fusions expressed under the respective native promoters. VapB-GFP was expressed under a constitu-

We investigated the interdependent localizations of the complex subunits by examining the subcellular distribution of each protein in the respective mutants. VapA localization in *vipC* or *vapB* mutants was the same as in the WT (not shown). VapB did not have an influence on VipC membrane localization. Lack of VapA, however, led to a loss of VipC signals at the plasma

membrane. Membrane localization of VapB was impaired not only in the *vapA* mutants but also in the *vipC* mutants, indicating that VipC plays a more important role in bridging the membrane-associated VapA to the methyltransferase VapB than vice versa. The VapB nuclear subpopulation increased in both the *vapA* and *vipC* mutants in comparison with the WT. VapB is primarily a nuclear protein without VapA (Figure 3C). Analysis of the protein levels in the mutants corresponded to the microscopic observations, with one exception: In the *vipC* mutant, a substantial amount of VapB remained in the nucleus although the overall VapB protein levels were reduced (Figure 3D), indicating that VipC protects VapB from degradation in the cytoplasm after it is released from the trimeric membrane complex and before it enters the nucleus.

The effect of the different subunits on complex formation was further elucidated in the mutants. In vivo associations of VipC were analyzed by TAP in the absence of VapA or VapB (Figure 3E). VipC-TAP recruited VapA and VapB in the WT, but the VipC-VapB interaction was abolished in the *vapA* mutant. BIFC studies of VipC-VapB methyltransferases also did not result in interaction signals in the *vapA* mutant (not shown). The VipC-VapA interaction was reduced in the *vapB* mutant. There is only a partial requirement of VapB for binding of VipC through VapA to the membrane, but VapA seems to be important to allow VipC-VapB heterodimer formation.

These results underscore that VapA is required for membrane assembly and release of VipC-VapB by an as yet unknown trigger. The VipC subunit presumably stabilizes VapB when the VipC-VapB methyltransferase migrates from the membrane into the nucleus.

Membrane-Associated VapA Prevents Developmental Control Functions of the VipC-VapB Methyltransferases

VipC is important for the appropriate adjustment of asexual or sexual programs in response to external cues, such as light, after the release of VipC-VapB from the membrane. VipC also interacts in the nucleus with VeA. The protein and transcript levels of VapA, VipC, and VapB were monitored for developmental responses to different stimuli. Submerged cultures resulted preferentially in vegetative growth, whereas illumination and darkness favored asexual spore formation and sexual development, respectively (Figure 4A). Each member of the complex was constantly expressed under all tested conditions, suggesting that physical interactions and their effects on activity, stability, and localization are more important than expression levels as a molecular control mechanism.

We compared the function of *vapA* or *vapB* genes for fungal development with that of *vipC* by analyzing corresponding deletants during illumination and darkness (Figure 4B). VapB is required even more than VipC to promote asexual and repress sexual development in light. The *vapB* mutant was blind to light and produced hardly any asexual spores, but formed constantly high numbers of sexual structures in light or darkness. Growth under different light spectra, including red (680 nm), blue (460 nm), and UVA (366 nm) resulted in the same light-unresponsive phenotype. A double deletion of the methyltransferase genes *vipC* and *vapB* displayed predominantly the *vapB* phenotype.

Whereas both methyltransferases VipC and VapB are required for asexual spore formation and light-dependent repression of sexual development, membrane-bound VapA has an antagonizing function. The *vapA* deletant produced 2.5 times more asexual conidia than the WT and formed significantly fewer sexual fruiting bodies. VapA is necessary to both repress asexual development and enhance sexual development. Double mutants of *vipC* and *vapB* with *vapA* exhibited an intermediate phenotype, showing no epistacy among the corresponding genes. The function of complex subunits for mycotoxin production was analyzed because development is linked to secondary metabolism. Except for some reduction in the *vipC*/*vapB* mutant, toxin levels did not change significantly (Figure 4C), indicating only a minor contribution of the methyltransferases to secondary metabolism control.

These findings support a molecular mechanism whereby, prior to an environmental trigger, VapA keeps VipC and VapB in a complex at the plasma membrane to prevent their developmental functions. Release of VipC-VapB into the nucleus promotes asexual development and decreases sexual development. This might include not only the nuclear methyltransferase activity of VipC-VapB but also the alternative nuclear VipC-VeA interaction.

Nuclear VipC-VapB Directs Transcription of Global Regulators for Asexual Development

The nuclear functions of VipC-VapB in controlling the light-dependent expression of regulatory genes to promote asexual (Figure 4D) or repress sexual development were examined. FlbA, a negative regulator of heterotrimeric G protein signaling, which is required for light-dependent activation of asexual development, activates a cascade of the transcription factors FlbC, BrlA, and AbaA to promote asexual sporulation (Park and Yu, 2012). Lack of VapA correlates with higher levels of nuclear VipC/VapB protein (Figure 3D) and increased expression of the downstream asexual regulatory genes *brlA* and *abaA.* There was also a less pronounced increase in transcripts for the upstream factors FlbA and FlbC (Figures 4D and S4). Transcripts of *veA*, *velB*, and *laeA* or the early sexual regulators *steA* and *nosA* (Vallim et al., 2000; Vienken and Fischer, 2006) were not seriously affected in the mutants (not shown). Membrane-bound VapA is primarily required for inhibiting transcription of asexual regulators and does not significantly affect sexual development regulators. The membrane location of VapA suggests an indirect inhibition function for VapA.

In contrast to a *vapA* deletion, the deletion of *vipC* and *vapB* did not increase transcription of *brlA* or *abaA*, and instead led to a decrease in *brlA* or *abaA* expression, which was more pronounced in the *vapB*/*vipC* double mutant (Figure S4). This suggests that VipC and VapB serve functions opposite to those of VapA and are important for the activation of asexual conidiation. Transcripts for VipC-VapA-VapB were not significantly altered in the respective deletants. The shift between membrane-bound VapA-VipC-VapB and nuclear VipC-VapB heteromers primarily acts by controlling the induction of asexual development, where light might be one of several environmental stimuli. Light-dependent inhibition of sexual development might not be a direct impact of nuclear VipC-VapB activity on gene expression.

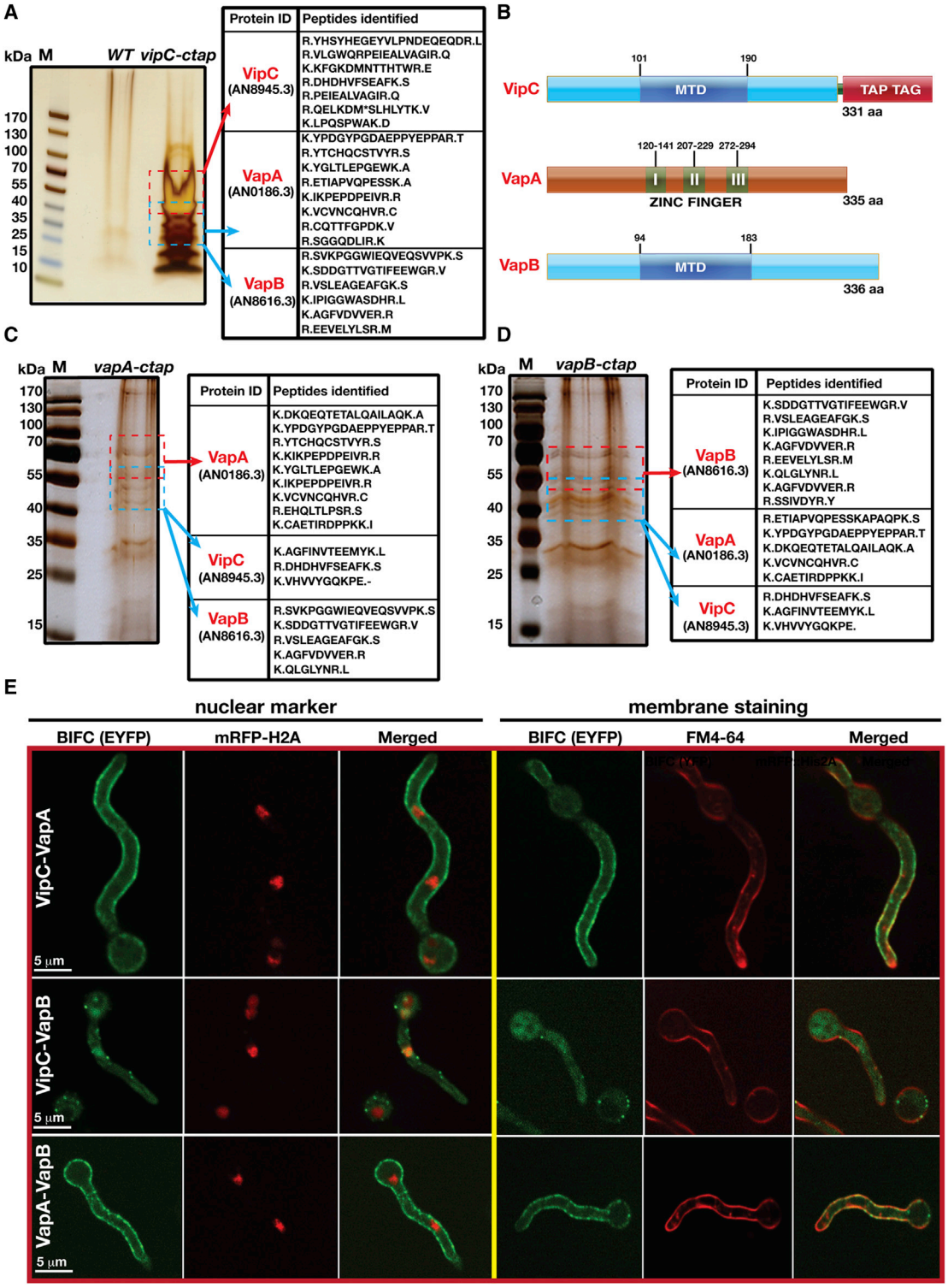

Figure 2. Trimeric Plasma Membrane-Associated VapA-VipC-VapB Releases the VipC-VapB Methyltransferase Heteromer to the Nucleus

(A) TAP of VipC-enriched proteins separated on 4%–15% silver-stained SDS-polyacrylamide gel. Polypeptides identified in mass spectrometry (MS) from TAP are given next to the gel (Table S1). Two VipC-associated proteins, VapA (AN0186.3) and VapB (AN8616.3), were identified.

(B) Domain architecture of VipC-associated proteins. MTD, methyltransferase domain including the SAM-binding site. Numbers indicate positions.

(C) Silver-stained 4%–15% SDS-polyacrylamide gel of VapA-TAP enrichment and identified polypeptides (Table S2). VapA recruits VipC methyltransferase and VapB.

(D) TAP of VapB interacting proteins VipC and VapA (Table S3).

(legend continued on next page)

Increased Cellular VipC-VapB Methyltransferase Protein Levels Influence Fungal Development and Secondary Metabolite Production

The equilibrium between nuclear and membrane-bound VipC-VapB controlled by VapA is important for the induction of asexual regulators. Light-dependent inhibition of sexual development might be an indirect effect of the release of VipC-VapB into the nucleus. Imbalanced cellular levels of these complexes should influence development, and we investigated this by overexpressing *vipC*, *vapA*, and *vapB* (Figure 5).

Overexpression of *vipC* or *vapB* methyltransferases repressed almost any differentiation in light, and reduced vegetative growth, asexual conidiation, and the formation of sexual fruiting bodies. In contrast, increased *vapA* levels resulted in colonies similar to the WT (Figures 5A and 5B). A more detailed analysis revealed differences between VipC and VapB functions. High levels of VipC caused defects in the nuclear distribution of germlings that accumulated many nuclei in the swollen spores (not shown). *vapB* overproduction induced a retardation and reduction in fruiting body formation, which is the opposite effect of the *vapB* deletion in sexual development (Figure 4B). High VapB levels also disturbed secondary metabolism, leading to secretion of a brown pigment into the medium and reduced asexual conidiation.

The interactions and subcellular locations of VapA, VipC, and VapB are interdependent. Without VapA, a VipC-GFP protein is unable to bind to the plasma membrane and to interact with the VapB methyltransferase. Overexpression of *vipC* or *vapB* in a *vapA* deletion or a deletion of the other methyltransferase gene did not cause significant developmental impacts. Similarly, dual overexpression of these two genes had no developmental effect, with the exception of concurrent overproduction of the methyltransferases VipC-VapB, which caused a further enhanced phenotype upon development that resembled a *veA* deletion strain without any fruiting bodies (Figures 5A and 5B).

A *veA* mutant is impaired in development and secondary metabolism (Kato et al., 2003; Kim et al., 2002), and VeA interacts with VipC (Figure 1A). Whereas the *vapB* deletant was not altered in secondary metabolism, *vapB* overexpression resulted in brown pigmentation. To investigate whether there are additional effects on secondary metabolism in overexpression strains, we measured ST mycotoxin levels. Toxin production was only abolished in the presence of high VapB levels or combined overexpression of VipC-VapB, whereas high VapA levels could suppress this phenotype (Figure 5C). We examined whether VapB and VipC methyltransferase activities were necessary for the observed effects. The SAM-binding motif was impaired by generating mutant alleles, *vipC1* and *vapB1* carrying a substitution of Gly (G) to Ala (A) in the SAM-binding motif. Overexpression of *vipC1* and *vapB1* abolished any effect on development and secondary metabolism observed in overexpression of the WT alleles (Figure S5).

The phenotypes of *vapB* overexpression correspond to a *veA* deletion. An examination of the impact of *vapB* overexpression on transcription of the nuclear VelB-VeA-LaeA complex (Figure 5D) revealed an almost 50% reduction in *laeA* or *veA*, but a 2-fold increase in *velB* transcripts. We investigated expression of the ST cluster genes controlled by the transcription factor AflR (Brown et al., 1996; Fernandes et al., 1998). *vapB* overexpression only slightly decreased expression of the regulatory *aflR* gene, but drastically reduced transcripts of *stcE*, *stcU*, and *stcQ* genes representing different locations in the cluster. Similar effects observed for the penicillin and terraquinone clusters corroborated the conclusion that *vapB* overexpression has a broad impact on secondary metabolism (Figure 5D).

Overexpression of *vapB* caused an opposite effect on the orsellinic acid gene cluster. A detailed examination of the overexpression strains revealed that the products of the orsellinic acid and its derivatives F9775A and F9775B were accumulated in *vapB* overexpression in a *vipC*-dependent manner (Figure S6). This is apparently due to the negative effect of *vapB* on *veA* gene expression, because deletion of *veA* results in an elevated expression of orsellinic acid gene cluster (Bok et al., 2013).

These results underline that VapA functions antagonistically to VipC-VapB, apparently by excluding them from the nucleus. Increased protein levels of VipC-VapB, which shift the ratio from membrane-associated VapA-VipC-VapB to more nuclear VipC-VapB, not only influences asexual and sexual development but has also an impact on secondary metabolism.

Membrane-Associated VapA Contributes to VeA Nuclear Import, which Is Reduced by VipC-VapB Methyltransferases

VipC physically interacts with VeA, and the VipC-VapB heteromer affects *veA* expression. The controlled import of VeA into the nucleus sets a threshold for coordination of development and secondary metabolism. Deletion of the *vapA* ZF gene prompts a drastic decrease in fruiting body formation and an increase in asexual conidiation. In contrast, strains lacking the methyltransferases show opposite phenotypes with elevated sexual but reduced asexual development. We addressed the nuclear import of VeA in the corresponding mutants. Subcellular localization of the functional VeA-GFP fusion expressed under the native promoter was monitored in the absence of VapA, VipC, or VapB. VeA-GFP was mostly targeted to the nucleus in the WT strains (Figure 6A). Lack of membrane-bound VapA resulted in increased cytoplasmic VeA, suggesting that VapA contributes to VeA nuclear import. When both VipC and VapB were absent, more VeA was enriched in the nucleus (Figure 6A). These findings were substantiated by the VeA protein levels in the respective mutants. VeA was equally expressed in the WT and mutants (Figure 6B). Enriched nuclear extracts revealed that the VeA nuclear import decreased in *vapA* but increased in the *vapB* and *vipC* mutants in comparison with the WT (Figure 6C).

VeA nuclear entry was also investigated in overexpression strains. *vapB* overexpression had a negative effect on *veA* transcripts levels, resulting in decreased sexual development and

(E) In vivo subcellular interactions of VipC-VapA, VipC-VapB, or VapA-VapB heterodimers by BIFC. VipC-VapA and VapA-VapB interact along the plasma membrane, and VipC-VapB interacts at membrane and in nuclei (visualized by mRFP-H2A fusion). FM4-64 dye stains plasma membrane red. Strains for TAP and BIFC were grown vegetatively for 24 hr and 16 hr, respectively, at 37°C in light.
See also Figures S1 and S2 and Tables S1, S2, and S3.

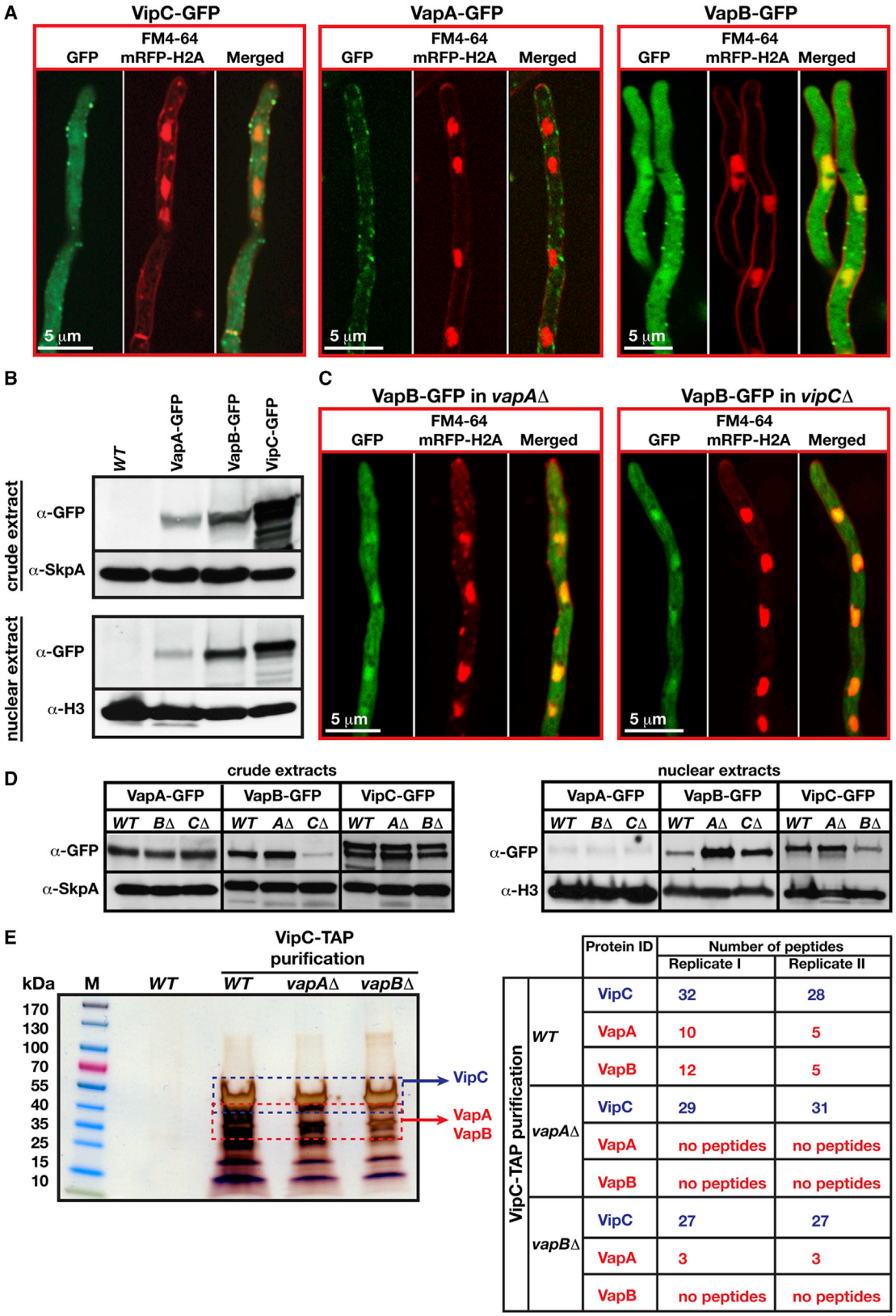

		Protein ID	Number of peptides	
			Replicate I	Replicate II
VipC-TAP purification	WT	VipC	32	28
		VapA	10	5
		VapB	12	5
	vapAΔ	VipC	29	31
		VapA	no peptides	no peptides
		VapB	no peptides	no peptides
	vapBΔ	VipC	27	27
		VapA	3	3
		VapB	no peptides	no peptides

(legend on next page)

impaired ST production. Overexpression of *vapB* led to reduced VeA nuclear localization (Figure 6D), but there was hardly any VeA-GFP fusion present in the cell (Figures 6E and 6F). VeA was predominantly found in nuclei when *vapA* or *vipC* were overexpressed, but the protein level of VeA was diminished in *vapB* overexpression.

The data suggest that VapA contributes to nuclear entry of VeA by keeping VipC and VapB at the membrane. VipC and particularly VapB reduce VeA nuclear import and protein levels, and there might be additional molecular mechanisms controlling VeA nuclear entry.

VeA Physically Interacts with VapB Methyltransferase

The initial finding of this study was the physical interaction between VipC and VeA. VapB impairs cellular VeA levels and negatively contributes to its nuclear import. We analyzed whether there are physical interactions between VapA or VapB MT and VeA. VapA did not interact with VeA in coIP and also did not result in a yellow fluorescent BIFC signal in the microscope (Figure 6G). VapB coprecipitated VeA similarly to VipC irrespective of illumination (Figures 6H and S7A). The BIFC localization signal indicated interaction within and at the border of the nucleus (Figure 6H). These results demonstrate that both VipC and VapB, but not VapA, physically interact with VeA at nuclear and perinuclear physical contact sites.

VapB Counteracts H3K9me3 and Controls Heterochromatin Distribution in the Nucleus

Nuclear VipC-VapB affects sexual development and, when overexpressed, secondary metabolism, presumably by interfering with VeA location and stability. Histone 3 undergoes extensive PTM, including methylation of various residues (Berger, 2007), and could be an additional target of nuclear VipC-VapB methyltransferase to control asexual development. Single or double mutants of the VapA-VipC-VapB complex did not lead to any changes in major histone marks, including H3K9me3 (repression), H3K4me2, and H3K9/K14 acetylation (activation). A significant effect was achieved by VapB overexpression, which resulted in a 50% reduction of H3K9me3 (Figure 7A), whereas other histone PTMs were not significantly altered. The VapB1 variant carrying an amino acid substitution in the SAM domain could not decrease H3K9me3, corroborating that the SAM-binding motif is crucial for H3K9me3 reduction and developmental function.

Heterochromatin protein HepA (HP1 in humans) binds to H3K9me3 histone marks to establish facultative heterochromatin (Maison and Almouzni, 2004). HepA-GFP fusion formed two to four distinct heterochromatin foci in the WT (Figure 7B). Overexpression of *vapB* resulted in a significantly different distribution of HepA signals diffused to the entire nucleus, implying that a subpopulation of nuclear VapB/VipC methyltransferase counteracts H3K9me3 modification. This is an additional nuclear function of VapB and VipC (besides their impact on the sexual program) that impairs VeA nuclear import and protein stability through direct physical interactions. An epigenetic methyltransferase activity of VapB might activate the regulatory genes for asexual conidiation, because repressive H3K9me3 marks increased, whereas competing H3K9/14ac marks decreased in *brlA* or *abaA* promoters in *vapB* and *vipC* mutants (Figure S7B). In contrast, a *vapA* deletion caused a decrease in H3K9me3 levels in these promoters, supporting a complex physical interplay between the developmental *velvet* domain protein VeA and epigenetic methyltransferases.

DISCUSSION

SAM is one of the most frequent cofactors in the cell after ATP, and SAM-dependent methyltransferases are involved in methylation of proteins, DNA, RNA, lipids, and small molecules. Protein and DNA methylations provide epigenetic control of gene expression in eukaryotes. The membrane-associated VapA-VipC-VapB fungal heterotrimeric protein complex includes the FYVE-like ZF protein VapA and the methyltransferase heteromer VipC-VapB. VapA is a positive regulator of sexual development when the methyltransferases are tethered to the membrane. Release of VipC-VapB from the membrane results in repression of sexual development and secondary metabolism. Nuclear methyltransferase VapB influences heterochromatin distribution by decreasing H3K9me3 and promoting the asexual differentiation program.

VapA-VipC-VapB and the *velvet* complex VelB-VeA-LaeA include the distinct SAM-dependent methyltransferase subunits VipC, VapB, and LaeA. The ZF VapA attaches the VipC-VapB methyltransferase heteromers to the membrane (Figure 7C). For *Velvet* complex formation, the cytoplasmic *velvet* domain heterodimer VeA-VelB must be imported to the nucleus, where it recruits LaeA. Both trimeric complexes are required to promote sexual development and secondary metabolism. External triggers such as light, nutrition, oxygen supply, and sexual hormones might affect the formation of both trimeric complexes. The VapA-VipC-VapB complex dissociates the methyltransferase dimers from the plasma membrane, resulting in a reduced *velvet* complex because the VipC-VapB dimer impairs VeA nuclear entry and stability. VeA is subject to complex PTMs

Figure 3. Subcellular Distribution of the VapA-VipC-VapB Complex Subunits

(A) Localization of VipC and VapA-GFP expressed under native and VapB under constitutive *gpdA* promoter. VipC and VapB are present at plasma membrane (red dye FM4-64) and within nuclei (mRFP-H2A) and VapA primarily at the plasma membrane.

(B) Functional VipC, VapA, and VapB GFP fusion levels in crude and nuclear extracts with significant nuclear VipC and VapB fractions; 50 μg crude and enriched nuclear extracts were used for immunoblottings with α-GFP, α-SkpA, and α-histone 3 (H3).

(C) Localization of VapB in *vapA* or *vipC* mutants in which membrane accumulation of VapB is impaired in the absence of VapA and VipC.

(D) Subcellular levels of VapB, which is enriched in the nucleus in the absence of VapA.

(E) TAP of VipC from *vapA* and *vapB* mutants. Silver-stained polyacrylamide gel of VipC TAP. VipC is unable to recruit VapB in the absence of VapA. The number of protein peptides identified by MS is next to the gel (Table S4). Strains for immunoblotting and TAP were grown for 24 hr, and strains for GFP localization were grown for 16 hr at 37°C in light.

See also Figure S3, Table S4, and Movie S1.

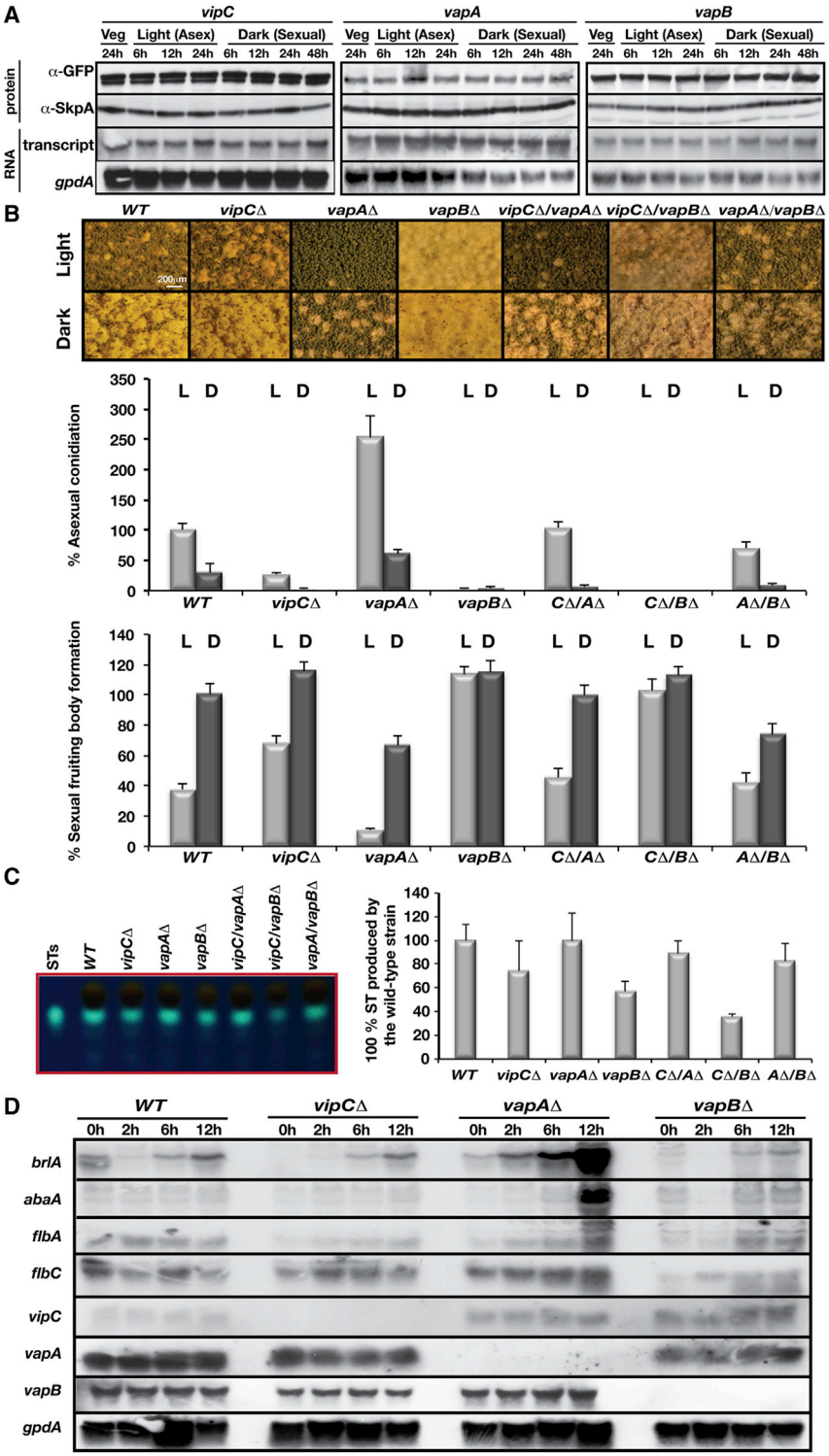

Figure 4. Expression and Light-Dependent Development of Genes for Membrane-Attached VapA-VipC-VapB or Nuclear VipC-VapB

(A) Protein and transcript levels of VipC, VapA, and VapB GFP fusions expressed under native promoter. After 20 hr of vegetative growth in liquid shaking GMM media, mycelia were transferred to solid GMM to induce differentiation in light for 6 hr, 12 hr, and 24 hr to induce asexual development, or in darkness for 6 hr, 12 hr, 24 hr, and 48 hr to induce sexual development. Proteins and RNAs were isolated at each time point. Proteins were detected with α-GFP. Loading controls: α-SkpA for proteins, *gpdA* for RNA.

(B) Fungal development. Stereomicroscopic images of phenotypes of WT, *vipC*Δ, *vapA*Δ, and *vapB*Δ single and double (*vipC*Δ/*vapA*Δ, *vipC*Δ/*vapB*Δ, and *vapA*Δ/*vapB*Δ) mutants grown on GMM for 5 days in light or darkness. Conidiation and fruiting body formation was quantified from five sectors from five plates; WT represents 100%. Vertical bars show SDs.

(C) ST production visualized on TLC plates. Vertical lines represent the error bars from two different TLC plates. STs, ST standard.

(D) Control of developmental regulatory genes by VapA-VipC-VapB. Cultures from *vipC*, *vapA*, or *vapB* mutants grown for 20 hr in GMM liquid shaking media and taken onto solid plates to propagate asexual development for 12 hr at 37°C in the light are shown. Total 20 μg RNA of indicated time points was loaded with *gpdA* as control. Asexual regulatory genes *brlA* and *abaA* are upregulated in the *vapA* mutant, whereas *flbA* or *flbC* are reduced in *vapB* and *vipC*.

See also Figure S4.

(Sarikaya Bayram et al., 2010). Nuclear VipC-VapB counteracts the trimethylation of H3K9, which in turn affects gene expression and activates asexual development.

To our knowledge, nuclear shuttling of membrane-tethered methyltransferases has not yet been described. Transmembrane methyl-accepting chemotaxis receptors of bacteria are controlled by CheR/CheB as a cytoplasmic methyltransferase and demethylase pair (Kentner and Sourjik, 2009). CheR homologs also control biofilm formation in pathogenic bacteria (García-Fontana et al., 2013). Catechol O-methyltransferases are membrane bound and contribute to O-methylation of catecholamine neurotransmitters as dopamine and norepinephrine in the human brain (Rivett et al., 1983). Protein arginine methyltransferases (PRMTs) of mammalian cells are associated with the plasma membrane. PRMT8 is directly tethered to the plasma membrane by amino-terminal myristoylation (Lee et al., 2005). Mammalian PRMTs can interact with transmembrane receptors such as interferon-α1, B cell antigen, and epidermal growth factor receptor (Yang and Bedford, 2013). Crosstalks between methyltransferase and MAPK signal transduction pathways include PRMT5, which influences RAS-ERK signal transduction. It also methylates RAF proteins, resulting in enhanced degradation of CRAF and BRAF (Andreu-Pérez et al., 2011).

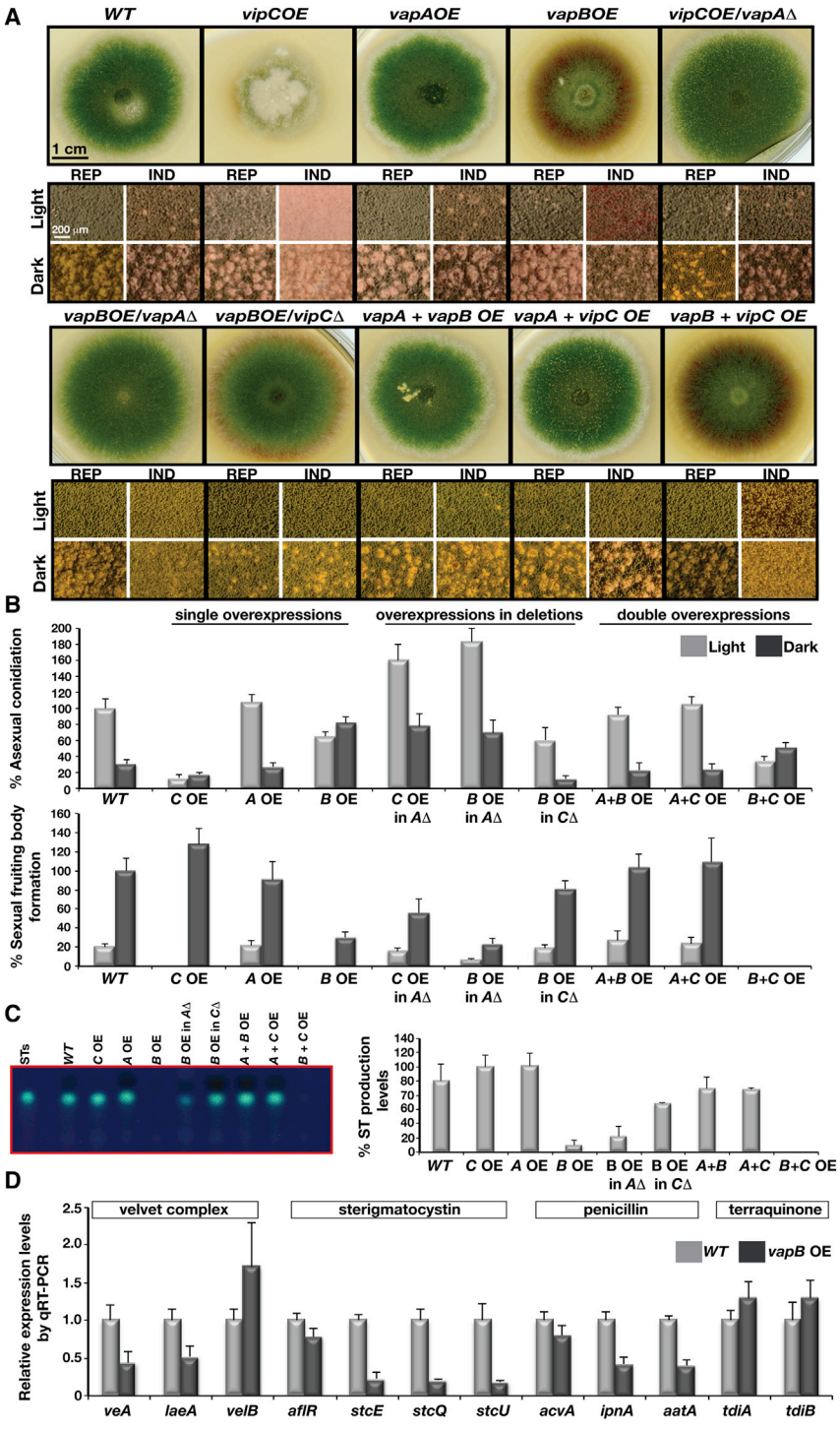

Figure 5. Overproduction of VipC-VapA-VapB and Their Developmental and Secondary-Metabolism Consequences

(A) Growth during *vipC*, *vapA*, and *vapB* overexpression (OE) under nitrogen-source inducible bidirectional *niiA-niiD* promoters in the WT or deletion strains. Development was induced on solid media after 5 days in light at 37°C. Stereomicroscopic images of growth on inducing or repressing media in light or darkness (enlarged squares).

(B) Quantification of asexual conidia and sexual fruiting body formations. Overexpression of VipC and VapB resulted in growth and developmental defects. Co-overexpression of VapA neutralized the influence of increased VipC and VapB. Conidia and fruiting bodies produced by the empty plasmid control are 100%. Vertical lines represent the error bars from five different plates for conidia and fruiting bodies.

(C) A TLC plate of ST production in the indicated OE strains. High *vapB* reduced ST levels when *vipC* was present. ST of the WT is 100%. Vertical lines represent the error bars from two different TLC plates.

(D) Real-time qPCR expression of *veA*, *laeA*, *velB*, and several structural genes for ST, penicillin, and terraquinone clusters in *vapB* OE strain.

See also Figures S5 and S6.

The fungal MAPK and VipC-VapB MT pathways communicate through VeA. This includes shifts in the ratio between nuclear and cytoplasmic distribution, stability, and phosphorylation of VeA, which makes it prone to interact with VelB and affect VeA function to control sexual development and secondary metabolism. LlmF represents a cytoplasmic LaeA-like methyltransferase that reduces the VeA nuclear import (Palmer et al., 2013). VipC-VapB interacts with VeA at the border and inside the nucleus. In the absence of VipC-VapB, nuclear accumulation of VeA increases, suggesting a role in nuclear entry. VeA nuclear import decreases in the *vapA* mutant, where VapB or VipC reduces nuclear VeA accumulation. Consistently, increased levels of VapB cause impaired sexual development and secondary metabolism. VeA interacts with numerous proteins that act as transcription factors, including the *velvet* family protein VelB (Ahmed et al., 2013). An increased interaction of VeA with VapB-VipC would allow VeA partners to participate in different complexes and affect asexual development. This might be a reason why VeA contributes to the expression of major asexual regulatory genes, such as *brlA* (Kato et al., 2003; Kim et al., 2002). VeA also acts as a repressor of the orsellinic acid gene cluster, and therefore reduced VeA (as in the case of VapB overexpression) leads to an accumulation of orsellinic acid derivatives.

A second nuclear function of VipC-VapB is epigenetic histone modification. Methylation and acetylation of H3K9 are competitive, and acetylation turns on gene expression. Methylation of histones has opposing functions depending on where the methylation occurs. Methylation of H3K4 often correlates with

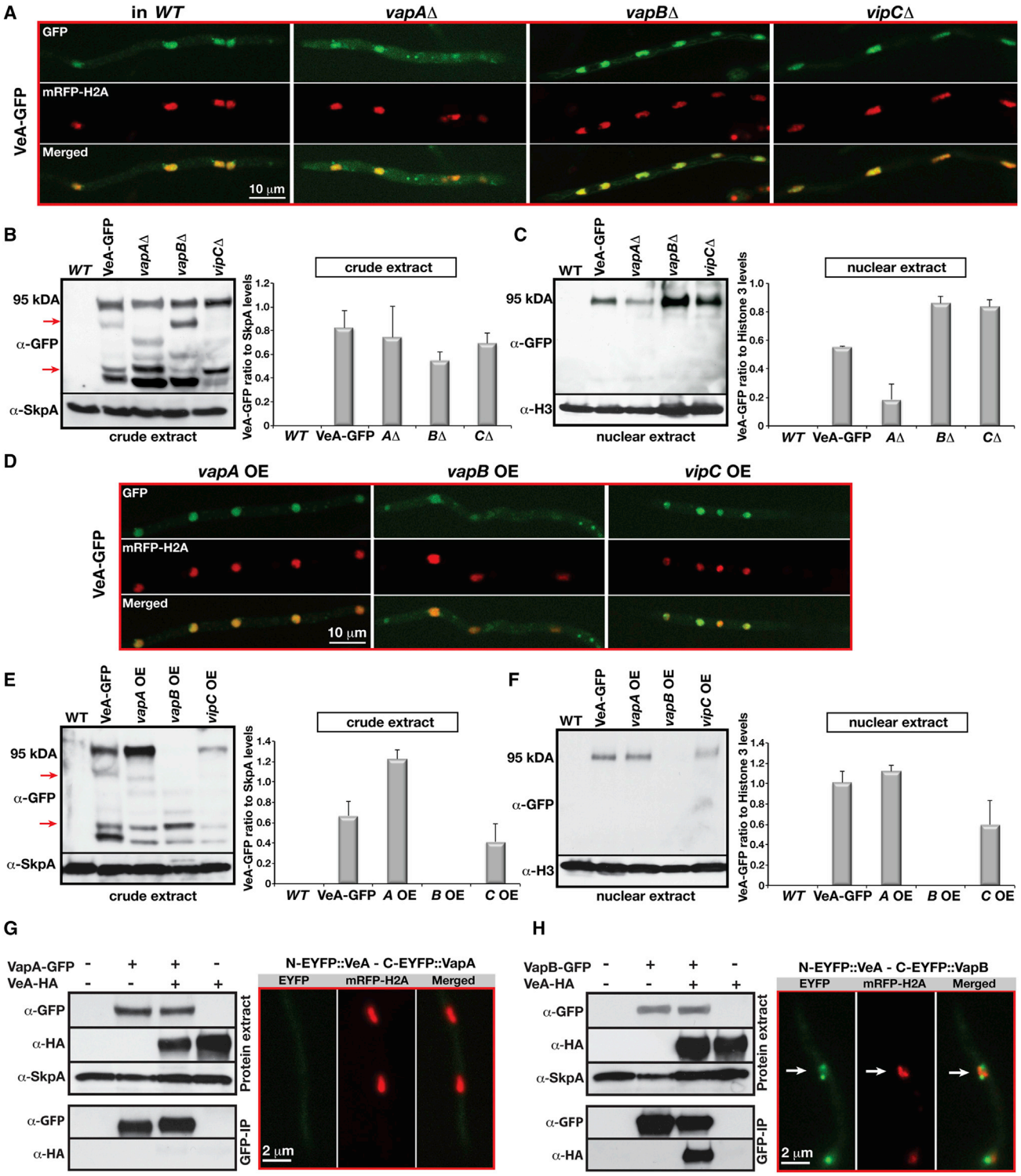

Figure 6. VapA and the Methyltransferases VipC and VapB Contribute to Subcellular Localization and Nuclear Import of the VeA Protein

(A) Confocal microscopic images of functional VeA-GFP fusion in WT, *vapA*, *vapB*, or *vipC* deletions where the cytoplasmic subpopulation of VeA increases in the *vapA* deletant.

(B) VeA-GFP levels in crude extracts of deletion strains. Red arrows mark degradation products of VeA-GFP. *A*Δ, *B*Δ, and *C*Δ represent *vapA*, *vapB*, and *vipC* deletions, respectively. Vertical lines are SDs from two biological replicates.

(C) Nuclear subpopulations of VeA-GFP from enriched nuclear extracts of WT and mutants. VeA nuclear import is reduced without *vapA* and increased in *vapB* or *vipC* mutants.

(legend continued on next page)

active transcription, whereas H3K9 methylation reflects gene silencing and heterochromatin accumulation (Maison and Almouzni, 2004). Increased VapB levels cause a reduction in repressive H3K9me3. It is unknown whether the influence of the VipC-VapB heteromer on histone modification is mediated by interfering with H3K9 methyltransferase ClrD activity or by enhancing specific demethylases for H3K9 residues.

To explore the potential of fungi to produce bioactive compounds, and to control the growth of human and plant fungal pathogens, it is essential to understand the regulation of fungal development and natural product biosynthesis. The VapA-VipC-VapB complex represents an additional layer of communication between the membrane and the fungal *velvet* domain proteins. The physical and functional connection between light receptors and the VapA-VipC-VapB complex, and the exact molecular mechanism by which the VipC-VapB methyltransferase interferes with VeA nuclear import and stability will be the focus of future research. It will be interesting to know whether the interconnections between methyltransferase and MAPK signaling modules observed in *A. nidulans* are also conserved in other members of the fungal kingdom or other eukaryotes, and what kind of roles they play during development, pathogenesis, and secondary metabolite production.

EXPERIMENTAL PROCEDURES

Strains, Culture, and Growth Conditions

The *A. nidulans* strains used and generated in this study are listed in Supplemental Experimental Procedures. AGB152, AGB551, AGB552, and AGB506 strains were employed as parental recipient strains for the transformation of plasmid and linear DNA molecules. The WT and transformants were grown in glucose minimal medium (GMM) containing either $NaNO_3$ or NH_4-L-tartrate as the nitrogen source. Recombinant plasmid molecules were propagated in either DH5α or MACH-1 (Invitrogen) recipient *Escherichia coli* strains grown in LB medium in the presence of antibiotics. *A. nidulans* and *E. coli* strains were cultured and transformed as previously described (Punt and van den Hondel, 1992; Sarikaya Bayram et al., 2010).

Real-Time Quantitative PCR

Total RNA was isolated by using RNeasy (QIAGEN) according to the provider's protocols. Following DNAase digestion, 800 ng RNA was applied for cDNA synthesis by using the QuantiTect Reverse Transcription kit (QIAGEN). A Mastercycler ep *realplex* (Eppendorf) and the RealMaster SYBR Rox master mix (5 Prime) were used for real-time quantitative PCRs (qPCRs) with the samples containing 50 ng template cDNA. All real-time qPCR experiments were carried out in duplicates or triplicates. Histone 2A levels were used as the standard for relative quantification of Δct values (Livak and Schmittgen, 2001).

Protein Extraction, Nuclear Enrichment, and Immunoblotting

Fungal mycelia were ground in a mechanical grinder MM400 (Retsch) filled with liquid nitrogen. Protein extracts were prepared by resuspending the pulverized mycelia in PEB (50 mM Tris [pH 7.6], 300 mM NaCl, 1 mM EDTA, 0.1% NP-40, 10% glycerol, 1 mM dithiothreitol). Nuclei were isolated (Palmer et al., 2008) and proteins were determined by Bradford assays.

Primary and secondary antibodies were applied in the following dilutions.

Polyclonal rabbit α-calmodulin binding peptide (CBP, 07-482; Millipore), 1:1,000 dilution in TBS with 5% nonfat milk, secondary antibody goat α-rabbit (sc-2006; Santa Cruz) 1:2,000 in TBS 5% milk.
Monoclonal α-GFP (GFP (B-2):Sc-9996; Santa Cruz) 1:1,000 dilution in TBS, containing 5% nonfat milk, secondary antibody goat α-mouse (115-035-003; Dianova) 1:2,000 in TBS 5% milk.
Monoclonal α-HA (H 3663; Sigma) 1:1,000 dilution in TBS 5% milk, secondary antibody same as for α-GFP.
Rabbit polyclonal α-SkpA (raised in Genescript) 1:2,000 in TBS 5% milk with 0.1% Tween-20, same secondary antibody for α-CBP.
Polyclonal α-H3 (ab1791, Abcam), H3K9/14 (pAb-005-050; Diagenode), 1:2,500 in PBS 5% BSA, same secondary antibody for α-CBP.
H3K9me3 (mAb-153-050; Diagenode), H3K4me2 (mAb-151-050; Diagenode), 1:2,500 in PBS 5% BSA, same secondary antibody as for α-GFP.

CoIPs

For in vivo interaction studies, GFP-Trap (Chromotek) agarose was used. Fungal mycelia were pulverized in liquid nitrogen and resuspended in PEB containing a protease inhibitor cocktail (Roche). Then 10 μl of GFP-Trap agarose was shortly resuspended and washed in 1 ml PEB. From each strain, 8 mg of total crude extract (1.5–2 ml) was incubated with 10 μl of prewashed GFP-Trap agarose for 4 hr at 4°C on a rotator. Beads were washed with 1.5 ml protein buffer three times and finally boiled in 40 μl 3× protein loading dye, and 5 μl was run on 4%–15% SDS polyacrylamide gel for detection.

Statistical Analysis and Quantifications

The statistical significance of the experimental results was calculated by paired t test (http://www.graphpad.com/quickcalcs/). Immunoblots were quantified with the use of ImageJ (National Institutes of Health; http://rsbweb.nih.gov/ij/).

TAP and Liquid Chromatography-Tandem Mass Spectrometry Analysis of VipC, VapA, and VapB Interacting Proteins

Fungal strains carrying the C-terminal TAP tag were grown in liquid GMM media for 24 hr at 37°C. The mycelia were filtered through miracloth, washed with 0.96% NaCl (w/v) containing 1 mM PMSF, and finally ground in liquid nitrogen. For each purification experiment, 6 × 15 ml ground mycelia were used. Preparation of the protein extracts and TAP purifications were performed as previously described (Bayram et al., 2012b), and 50 ml of the protein extracts was subjected to TAP purification. The final eluates of the TAP purifications were precipitated and concentrated. They were separated on 4%–15% SDS polyacrylamide gels stained with either Coomassie brilliant blue or silver reagent. After trypsin digestion, peptides were analyzed with an LCQ DecaXP (Thermo Finnigan) mass spectrometer by using the TurboSEQUEST algorithm as previously described (Bayram et al., 2008). Identified proteins were further analyzed in the Aspergillus Genome Database (http://www.aspgd.org).

ACCESSION NUMBERS

The NCBI accession number for the *vapB* cDNA data reported in this paper is KJ572117.

SUPPLEMENTAL INFORMATION

Supplemental Information includes Supplemental Experimental Procedures, seven figures, four tables, and one movie and can be found with this article online at http://dx.doi.org/10.1016/j.devcel.2014.03.020.

(D) Confocal images of VeA-GFP in OE strains. Nuclear VeA-GFP localization is affected by high VapB.
(E and F) VeA in crude or nuclear extracts of WT and the respective OE. High *vapB* reduces *veA* transcript and VeA-GFP levels.
(G) Lack of in vivo interaction between VapA-VeA protein by coIP or BIFC.
(H) Interaction of VapB-VeA in CoIP or BIFC. GFP-TRAP was used for immunoprecipitations. VapB-VeA proteins interact at the edge and in the nucleus. Strains for GFP immunoblotting and coIP experiments were grown for 24 hr at 37°C in darkness, and BIFC or GFP strains were grown for 16 hr.
See also Figure S7.

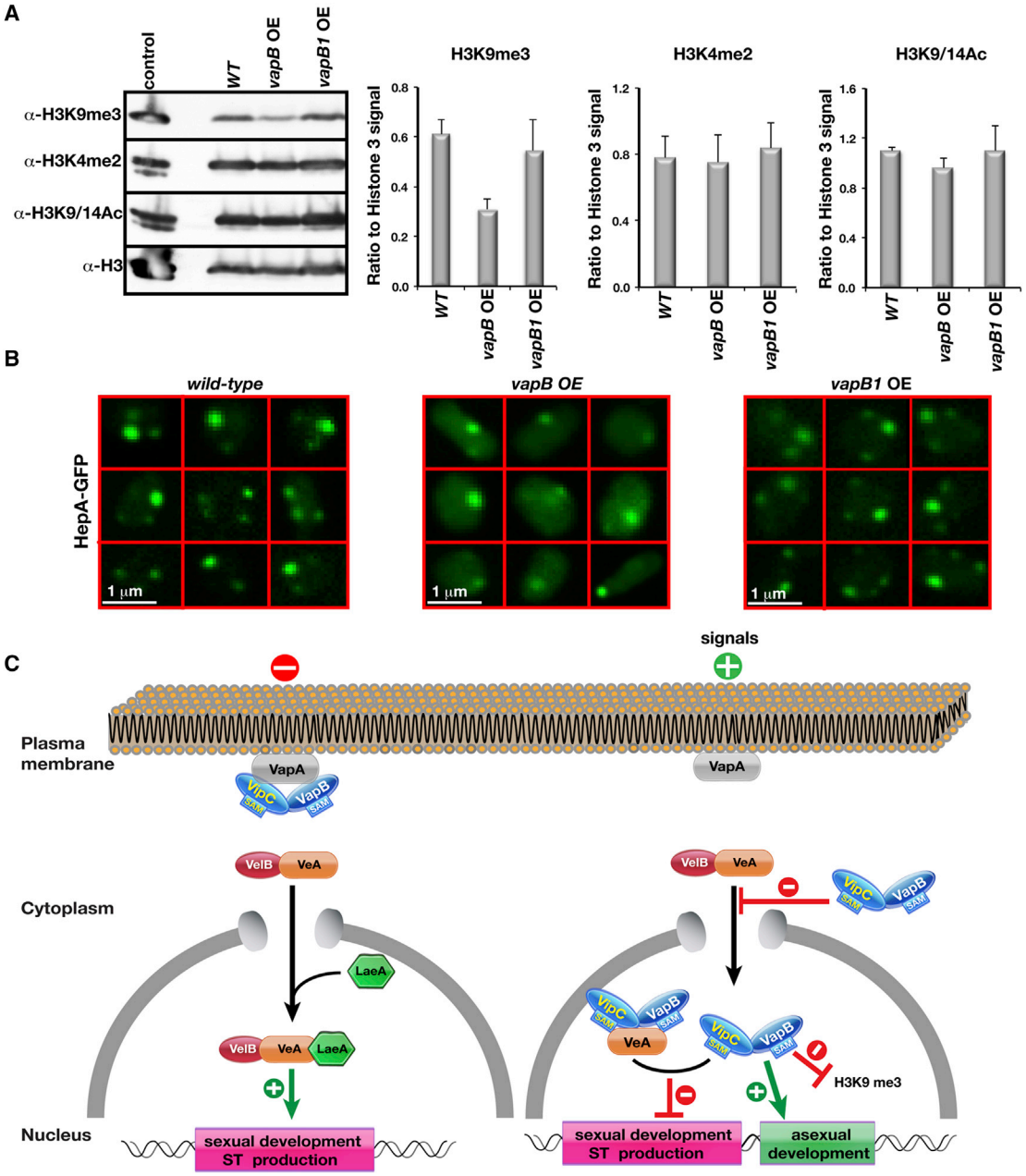

Figure 7. VapB-Mediated Posttranslational Histone 3 Modifications and Model of the Interplay between Trimeric VapA-VipC-VapB and VelB-VeA-LaeA Methylase Complexes

(A) Influence of VapB overexpression on histone 3 modification. Immunoblotting of enriched nuclei from WT, *vapB*, and *vapB1* OE strains with specific antibodies against H3K9me3, H3K4me2, H3K9/14 acetylation, and unmodified histone 3 quantified from two immunoblotting replicates. Vertical bars represent SDs. Nuclei of chicken erythrocytes served as controls.

(B) Nuclear distribution of heterochromatin (HepA-GFP) protein. HepA-GFP was expressed under endogenous promoter in WT, *vapB*, and *vapB1* grown for 24 hr at 37°C in light. Enlarged confocal images of nine different nuclei are shown.

(C) Model for VapA-VipC-VapB control of development and ST production. VapA-VipC-VapB assembles at the plasma membrane without external signal, allowing VeA-VelB to enter the nucleus and recruit LaeA to promote sexual development and secondary metabolism. External signals release VipC-VapB, which associates with VeA and reduces nuclear import, represses sexual development, and induces asexual conidiation by counteracting H3K9me3.

See also Figure S7.

ACKNOWLEDGMENTS

We thank Dr. Valerius for help with MS, Dr. Irmer for real-time qPCR advice, and Dr. Chen, Yogesh Ostwal, and Rafael Jaimes for ChIP suggestions. This study was funded by the DFG (SFB860 and SPP1365 to G.H.B.) and the National Research Foundation of Korea (NRF-2007-0053567 to D.M.H. and NRF-2011-0014718 to J.H.K.). It was also supported by Excellence Initiative FL3 INST 186/822-1 to I.F. and partly supported by Woosuk University.

Ö.S.-B. received an Excellence stipend from the Göttingen Graduate School for Neurosciences and Molecular Biosciences.

Received: October 6, 2013
Revised: February 26, 2014
Accepted: March 25, 2014
Published: May 27, 2014

REFERENCES

Ahmed, Y.L., Gerke, J., Park, H.S., Bayram, O., Neumann, P., Ni, M., Dickmanns, A., Kim, S.C., Yu, J.H., Braus, G.H., and Ficner, R. (2013). The velvet family of fungal regulators contains a DNA-binding domain structurally similar to NF-κB. PLoS Biol. *11*, e1001750.

Andreu-Pérez, P., Esteve-Puig, R., de Torre-Minguela, C., López-Fauqued, M., Bech-Serra, J.J., Tenbaum, S., García-Trevijano, E.R., Canals, F., Merlino, G., Avila, M.A., and Recio, J.A. (2011). Protein arginine methyltransferase 5 regulates ERK1/2 signal transduction amplitude and cell fate through CRAF. Sci. Signal. *4*, ra58.

Bayram, O., and Braus, G.H. (2012). Coordination of secondary metabolism and development in fungi: the velvet family of regulatory proteins. FEMS Microbiol. Rev. *36*, 1–24.

Bayram, O., Krappmann, S., Ni, M., Bok, J.W., Helmstaedt, K., Valerius, O., Braus-Stromeyer, S., Kwon, N.J., Keller, N.P., Yu, J.H., and Braus, G.H. (2008). VelB/VeA/LaeA complex coordinates light signal with fungal development and secondary metabolism. Science *320*, 1504–1506.

Bayram, O., Braus, G.H., Fischer, R., and Rodriguez-Romero, J. (2010). Spotlight on *Aspergillus nidulans* photosensory systems. Fungal Genet. Biol. *47*, 900–908.

Bayram, O., Bayram, O.S., Ahmed, Y.L., Maruyama, J., Valerius, O., Rizzoli, S.O., Ficner, R., Irniger, S., and Braus, G.H. (2012a). The *Aspergillus nidulans* MAPK module AnSte11-Ste50-Ste7-Fus3 controls development and secondary metabolism. PLoS Genet. *8*, e1002816.

Bayram, O., Bayram, O.S., Valerius, O., Jöhnk, B., and Braus, G.H. (2012b). Identification of protein complexes from filamentous fungi with tandem affinity purification. Methods Mol. Biol. *944*, 191–205.

Berger, S.L. (2007). The complex language of chromatin regulation during transcription. Nature *447*, 407–412.

Bi, Q., Wu, D., Zhu, X., and Gillian Turgeon, B. (2013). *Cochliobolus heterostrophus* Llm1—a Lae1-like methyltransferase regulates T-toxin production, virulence, and development. Fungal Genet. Biol. *51*, 21–33.

Bok, J.W., and Keller, N.P. (2004). LaeA, a regulator of secondary metabolism in *Aspergillus spp*. Eukaryot. Cell *3*, 527–535.

Bok, J.W., Soukup, A.A., Chadwick, E., Chiang, Y.M., Wang, C.C., and Keller, N.P. (2013). VeA and MvlA repression of the cryptic orsellinic acid gene cluster in *Aspergillus nidulans* involves histone 3 acetylation. Mol. Microbiol. *89*, 963–974.

Brakhage, A.A. (2013). Regulation of fungal secondary metabolism. Nat. Rev. Microbiol. *11*, 21–32.

Brown, D.W., Yu, J.H., Kelkar, H.S., Fernandes, M., Nesbitt, T.C., Keller, N.P., Adams, T.H., and Leonard, T.J. (1996). Twenty-five coregulated transcripts define a sterigmatocystin gene cluster in *Aspergillus nidulans*. Proc. Natl. Acad. Sci. USA *93*, 1418–1422.

Fernandes, M., Keller, N.P., and Adams, T.H. (1998). Sequence-specific binding by *Aspergillus nidulans* AflR, a C6 zinc cluster protein regulating mycotoxin biosynthesis. Mol. Microbiol. *28*, 1355–1365.

García-Fontana, C., Reyes-Darias, J.A., Muñoz-Martínez, F., Alfonso, C., Morel, B., Ramos, J.L., and Krell, T. (2013). High specificity in CheR methyltransferase function: CheR2 of *Pseudomonas putida* is essential for chemotaxis, whereas CheR1 is involved in biofilm formation. J. Biol. Chem. *288*, 18987–18999.

Gaullier, J.M., Simonsen, A., D'Arrigo, A., Bremnes, B., Stenmark, H., and Aasland, R. (1998). FYVE fingers bind PtdIns(3)P. Nature *394*, 432–433.

Gillooly, D.J., Simonsen, A., and Stenmark, H. (2001). Cellular functions of phosphatidylinositol 3-phosphate and FYVE domain proteins. Biochem. J. *355*, 249–258.

Good, M.C., Zalatan, J.G., and Lim, W.A. (2011). Scaffold proteins: hubs for controlling the flow of cellular information. Science *332*, 680–686.

Hayakawa, A., Hayes, S., Leonard, D., Lambright, D., and Corvera, S. (2007). Evolutionarily conserved structural and functional roles of the FYVE domain. Biochem. Soc. Symp. 95–105.

Hong, E., Lim, Y., Lee, E., Oh, M., and Kwon, D. (2012). Tissue-specific and age-dependent expression of protein arginine methyltransferases (PRMTs) in male rat tissues. Biogerontology *13*, 329–336.

Kato, N., Brooks, W., and Calvo, A.M. (2003). The expression of sterigmatocystin and penicillin genes in *Aspergillus nidulans* is controlled by *veA*, a gene required for sexual development. Eukaryot. Cell *2*, 1178–1186.

Keller, N.P., Turner, G., and Bennett, J.W. (2005). Fungal secondary metabolism—from biochemistry to genomics. Nat. Rev. Microbiol. *3*, 937–947.

Kentner, D., and Sourjik, V. (2009). Dynamic map of protein interactions in the Escherichia coli chemotaxis pathway. Mol. Syst. Biol. *5*, 238.

Kim, H., Han, K., Kim, K., Han, D., Jahng, K., and Chae, K. (2002). The *veA* gene activates sexual development in *Aspergillus nidulans*. Fungal Genet. Biol. *37*, 72–80.

Kozbial, P.Z., and Mushegian, A.R. (2005). Natural history of S-adenosylmethionine-binding proteins. BMC Struct. Biol. *5*, 19.

Lee, J., Sayegh, J., Daniel, J., Clarke, S., and Bedford, M.T. (2005). PRMT8, a new membrane-bound tissue-specific member of the protein arginine methyltransferase family. J. Biol. Chem. *280*, 32890–32896.

Livak, K.J., and Schmittgen, T.D. (2001). Analysis of relative gene expression data using real-time quantitative PCR and the 2(-Delta Delta C(T)) method. Methods *25*, 402–408.

Maison, C., and Almouzni, G. (2004). HP1 and the dynamics of heterochromatin maintenance. Nat. Rev. Mol. Cell Biol. *5*, 296–304.

Palmer, J.M., Perrin, R.M., Dagenais, T.R., and Keller, N.P. (2008). H3K9 methylation regulates growth and development in *Aspergillus fumigatus*. Eukaryot. Cell *7*, 2052–2060.

Palmer, J.M., Theisen, J.M., Duran, R.M., Grayburn, W.S., Calvo, A.M., and Keller, N.P. (2013). Secondary metabolism and development is mediated by LlmF control of VeA subcellular localization in *Aspergillus nidulans*. PLoS Genet. *9*, e1003193.

Park, H.S., and Yu, J.H. (2012). Genetic control of asexual sporulation in filamentous fungi. Curr. Opin. Microbiol. *15*, 669–677.

Patananan, A.N., Palmer, J.M., Garvey, G.S., Keller, N.P., and Clarke, S.G. (2013). A novel automethylation reaction in the *Aspergillus nidulans* LaeA protein generates S-methylmethionine. J. Biol. Chem. *288*, 14032–14045.

Punt, P.J., and van den Hondel, C.A. (1992). Transformation of filamentous fungi based on hygromycin B and phleomycin resistance markers. Methods Enzymol. *216*, 447–457.

Purschwitz, J., Müller, S., and Fischer, R. (2009). Mapping the interaction sites of *Aspergillus nidulans* phytochrome FphA with the global regulator VeA and the White Collar protein LreB. Mol. Genet. Genomics *281*, 35–42.

Rivett, A.J., Francis, A., and Roth, J.A. (1983). Localization of membrane-bound catechol-O-methyltransferase. J. Neurochem. *40*, 1494–1496.

Rodriguez-Romero, J., Hedtke, M., Kastner, C., Müller, S., and Fischer, R. (2010). Fungi, hidden in soil or up in the air: light makes a difference. Annu. Rev. Microbiol. *64*, 585–610.

Saito, H. (2010). Regulation of cross-talk in yeast MAPK signaling pathways. Curr. Opin. Microbiol. *13*, 677–683.

Sarikaya Bayram, O., Bayram, O., Valerius, O., Park, H.S., Irniger, S., Gerke, J., Ni, M., Han, K.H., Yu, J.H., and Braus, G.H. (2010). LaeA control of velvet family

regulatory proteins for light-dependent development and fungal cell-type specificity. PLoS Genet. *6*, e1001226.

Stinnett, S.M., Espeso, E.A., Cobeño, L., Araújo-Bazán, L., and Calvo, A.M. (2007). *Aspergillus nidulans* VeA subcellular localization is dependent on the importin alpha carrier and on light. Mol. Microbiol. *63*, 242–255.

Vallim, M.A., Miller, K.Y., and Miller, B.L. (2000). Aspergillus SteA (sterile12-like) is a homeodomain-C2/H2-Zn+2 finger transcription factor required for sexual reproduction. Mol. Microbiol. *36*, 290–301.

Vienken, K., and Fischer, R. (2006). The Zn(II)2Cys6 putative transcription factor NosA controls fruiting body formation in *Aspergillus nidulans*. Mol. Microbiol. *61*, 544–554.

Yang, Y., and Bedford, M.T. (2013). Protein arginine methyltransferases and cancer. Nat. Rev. Cancer *13*, 37–50.

Zheng, C.F., and Guan, K.L. (1993). Cloning and characterization of two distinct human extracellular signal-regulated kinase activator kinases, MEK1 and MEK2. J. Biol. Chem. *268*, 11435–11439.